

Theoretical understanding of SnS monolayer as Li ion battery anode material



Fangfang Wang^{a,b,1}, Qiushi Yao^{c,1}, Liyu Zhou^b, Zhen Ma^b, Mingxue He^b, Fang Wu^{a,b,*}

^a School of Science, Nanjing Forestry University, Nanjing, Jiangsu, 210037, PR China

^b College of Information Science and Technology, Nanjing Forestry University, Nanjing, Jiangsu, 210037, PR China

^c Department of Applied Physics, Nanjing University of Science and Technology, Nanjing, Jiangsu, 210094, PR China

ABSTRACT

Ideal Li-ion battery materials should have a low Li-ion diffusion barrier and a suitable binding energy. Here, first-principles calculations were performed to investigate the potential of SnS monolayer as a Li-ion battery material. Our study reveals that Li ions can be strongly bonded on the SnS monolayer with a binding energy of around 2 eV, and donate electrons into the SnS monolayer. Consequently, Li intercalation of SnS monolayer gives rise to a semiconducting to metallic transition, and leads to a good electrical conductivity. Interestingly, in spite of the existence of strong chemical interaction, the energy barrier (0.45 eV) of Li diffusion on the SnS monolayer is quite low. Moreover, the estimated open circuit voltage is about 1.98 V, which is much better than that of commercial graphite. Thus, given these advantages, it is expected that SnS monolayer will be a promising anode material for Li ion batteries.

1. Introduction

With the rapid development of consumer electronics, rechargeable supercapacitors/batteries with high capacity and rate capacity have attracted great attention from both basic research and industry applications [1–7]. Li-ion batteries (LIBs), one of the most widely studied rechargeable batteries, are in high demand in the portable electronics market, and their applications have expanded into large-scale electric energy storage, such as in renewable power stations and hybrid electric vehicles, because of their high specific-capacity density and stable cycling capability [4–7]. Currently, graphite-based carbon materials are widely used as the commercial anode materials for LIBs due to their unique electrochemical and physical properties [4]. However, developing LIBs with much better performance is always one of the hottest research topics [5–7]. On the other hand, the slow charging/discharging rate of present-day LIBs has limited further applications of LIBs in real devices. Although large current rates may help the charging rate, it may lead to fast decay of LIBs and safety problems. Generally, the charging/discharging process of LIBs can be divided into three steps: detachment from reservoir, transport in electrolyte, and diffusion in the electrodes. In this sense, finding a suitable anode, which has fast Li-ion diffusion, may provide an easy way to accelerate the charging/discharging rates.

Previously, many theoretical studies have shown that lowering the dimensionality of conventional anode materials via nanotechnology can achieve higher capacity [8]. For instance, materials with low dimensionality, such as fullerene [9,10], carbon nanotubes [11–13], silicon/germanium nano-wires [14–16], and graphene [17–23] have been intensively investigated for their potential as a replacement for graphite as anode. Among them, graphene has attracted immense attention because of its 2D crystal structure with atomic thickness, unique electronic structure, high intrinsic mechanical strength, high thermal conductivity, and large surface area [24,25]. Unfortunately, lithium nucleation over graphene limits its application in terms of durability [26]. Recent experimental studies demonstrated that monolayer phosphorene is a promising anode material for LIBs [27–29]. Li atoms form strong binding with phosphorus atoms, and the energy barrier of Li diffusion on monolayer phosphorene along the zigzag direction is only 0.08 eV, which leads to an ultrahigh diffusivity. According to the calculated energy barrier, the diffusivity is estimated to be 10^2 (10^4) times faster than that on MoS₂ (graphene) at room temperature [28]. However, phosphorene is not stable under ambient conditions, and degrades in air via light-induced oxidation. Considering their potential in LIBs, it is necessary to find an alternative way to get around this problem. Until now, it has not been clear whether the puckered structure of phosphorus plays the dominant role in the electrode of LIBs. Therefore, it is

* Corresponding author. School of Science, Nanjing Forestry University, Nanjing, Jiangsu, 210037, PR China.

E-mail address: fangwu@mail.ustc.edu.cn (F. Wu).

¹ These authors contributed equally.

quite interesting to explore the possibility of anode materials with similar structures.

Very recently, a new semiconductor material named herzenbergite SnS has attracted great interest. Herzenbergite SnS is composed of earth abundant elements and is relatively nontoxic [30]. The structure of herzenbergite SnS is layered, consisting of strong Sn-S bonds within a puckered sheet, and weak intermolecular interactions between the layers that is similar in structure to that of black phosphorus (BP) [31,32]. The 2D SnS monolayer can be mechanically exfoliated from the layered bulk herzenbergite. Similar to phosphorene, the atomic layered SnS nanomaterial has stacked puckered 2D honeycomb layers [33,34]. Although tin compounds such as tin metal, tin oxides, and tin sulfides with high theoretical gravimetric capacity and eco-friendliness are promising alternative anode materials [35–42], there are major drawbacks associated with these materials, including rapid deterioration and low retention of capacity, mainly originating from their high volume changes during charge–discharge cycling [42]. To resolve this issue, 0D nanoparticles, 1D nanowires/nanotubes, 2D nanosheets, and 3D core–shell/yolk–shell spheres of these electroactive Sn-based materials have been designed and fabricated to improve cyclic performance and achieve high Li-ion storage [35–42]. However, only a small number of studies have been carried out on tin sulfides compared to their oxides because of their lower microstructural flexibility [39–42]. In comparison with the disulfide of SnS₂, SnS shows high electrical conductivity (0.193–0.0083 S cm⁻¹) [43,44], indicating that SnS is a promising anode material. Previously, SnS has been proved to be a potential LIB material in experiments; however, theoretical understanding has still not been explored [44].

In this study, we employ first-principles calculations based on density functional theory (DFT) to investigate the adsorption and diffusion of Li on the SnS monolayer in order to assess the suitability of the SnS monolayer as a host material in LIBs. Our calculations indicate that Li atoms bind more strongly on SnS monolayer than on monolayer graphene. The diffusion barrier values of the Li atoms are calculated as approximately 0.45 eV on an SnS monolayer, which is a suitable diffusion barrier for LIBs. The calculated open-circuit-voltage average value is around 1.98 V, which is obviously higher than those of graphite [45] and TiO₂ electrodes [46], for which the average voltage is around 1.5 V. Thus, the SnS monolayer-based Li battery is able to provide a much higher charging voltage. These results suggest that SnS monolayer holds great potential for use in LIBs.

2. Calculation methods

Our first-principles calculations were based on DFT with generalized gradient approximation (GGA) [47] for exchange correlation potential. Perdew-Burke-Ernzerhof (PBE) functional was used for the GGA as implemented in Vienna ab initio simulation package (VASP) [48]. A 3 × 3 × 1 supercell was used to simulate Li adsorption on the SnS monolayer. The distance between two adjacent Li atoms was around 10 Å, which can avoid the interactions between two Li atoms. Also, a vacuum space of about 15 Å between SnS layers was used to avoid any interactions. The structures were relaxed without any symmetry constraints and a cutoff energy of 500 eV. The convergence criteria of energy and force were set to 1 × 10⁻⁵ eV and 0.01 eV/Å, respectively. Reciprocal space was represented by a Monkhorst-Pack special k-point scheme [49] with 3 × 3 × 1 grid meshes for structure relaxation for SnS monolayer. Self-consistent field (SCF) computations were performed with k-points of 5 × 5 × 1 grid meshes for SnS monolayer. By placing Li atoms at a different site, and relaxing the structure, the binding energy per atom for the adsorption of n Li atoms is defined as

$$E_b = (E_{\text{SnS}+n\text{Li}} - E_{\text{SnS}} - nE_{\text{Li}})/n \quad (1)$$

where E_b is the binding energy of Li on SnS monolayer, E_{SnS} is the energy of SnS monolayer supercell without Li atom, E_{Li} is the energy of isolated Li atom, and $E_{\text{SnS}+n\text{Li}}$ is the total energy of SnS monolayer with

adsorbed n Li atoms. According to this definition, a more negative value of E_b indicates a more energetically favorable (exothermic) reaction. To denote the concentration of Li on the SnS monolayer, we use the notation of Li_xSnS, as in previous studies. To obtain the open circuit voltage (OCV) [50], we considered the reaction



where x is the number of adatoms inserted in the per SnS molecular. The electronic potential during this process can be written in the form of Gibbs free energy

$$V = -\frac{\Delta G_f}{zF},$$

where z and F are the number of valence electrons during the adatom process and the Faraday constant, respectively; ΔG_f is the change in Gibbs free energy during the adatom process which is defined as

$$\Delta G_f = \Delta E_f + P\Delta V_f - T\Delta S_f,$$

$P\Delta V_f$ is on the order of 10⁻⁵ eV and the term $T\Delta S_f$ is comparable to 26 meV at room temperature; thus, the entropy and pressure terms are negligible [50]. ΔG_f is then approximately equal to the formation energy, ΔE_f , involved in the adsorption process, which is defined as

$$\Delta E_f = E_{\text{Li}_x\text{SnS}} - (E_{\text{SnS}} + xE_{\text{Li}}),$$

where $E_{\text{Li}_x\text{SnS}}$ is the total energy of the composite system with x metal atoms adsorbed in the per SnS molecular, E_{Li} is the total energy of a single Li in a bulk BCC structure and E_{SnS} is the total energy of an isolated SnS. The OCV is related to the formation energy by

$$\text{OCV} = \frac{\Delta G_f}{x} \approx \frac{\Delta E_f}{x} \quad (2)$$

The climbing image nudged elastic band (NEB) [51,52] was performed to find saddle points and minimum energy paths (MEPs) between a given initial state (IS) and final state (FS). The NEB method is known as an effective tool for finding MEP and transition state (TS) [53,54].

3. Results and discussion

As shown in Fig. 1, SnS is a layered puckered structure with weak van der Waals (vdW) forces, which resembles BP. Similar to phosphorene, the 2D SnS monolayer was mechanically exfoliated from the layered 3D bulk parent. As depicted in Fig. 1d, the calculated band dispersion with PBE method shows that 2D SnS monolayer is an indirect semiconductor with a band gap of 1.42 eV. In contrast to phosphorene, the conductive band minimum (CBM) is contributed by Sn ions, while the valence band maximum (VBM) is dominated by S ions. The calculated partial charge densities are closely related to the local chemical bonding within the structures. For phosphorene, there is a strong s-p hybridization, forming covalent bonding between P atoms. However, for SnS, ionic bonding is favored between Sn and S atoms, leading to the strong electron transfer, which is confirmed by the charge density plot. Consequently, the calculated band gap is much larger in SnS than that in phosphorene.

Next, we studied the possibility of single Li atom adsorption on SnS monolayer. To avoid the interaction of Li atoms, we adopted a 3 × 3 × 1 supercell of the SnS monolayer. According to the symmetry of the crystal structure, there are four possible sites for Li atoms on SnS monolayer, namely, the top site of an S atom (T_S), on an Sn atom (T_{Sn}), the bridge site over an S-Sn bond (B), and the hollow site of a hexagon ring (H), as shown in Fig. 2. By placing Li atoms at a possible site, and relaxing the structure, we find that the Li atoms on T_{Sn} or T_S site prefer to stay at the H site, and while the Li atom is initially placed on the B site, after structural relaxation, the Li atom will spontaneously move to the H_B site. Thus, it is natural to question whether the banding energy of Li atom doping on H site is different from that on H_B site. To find the

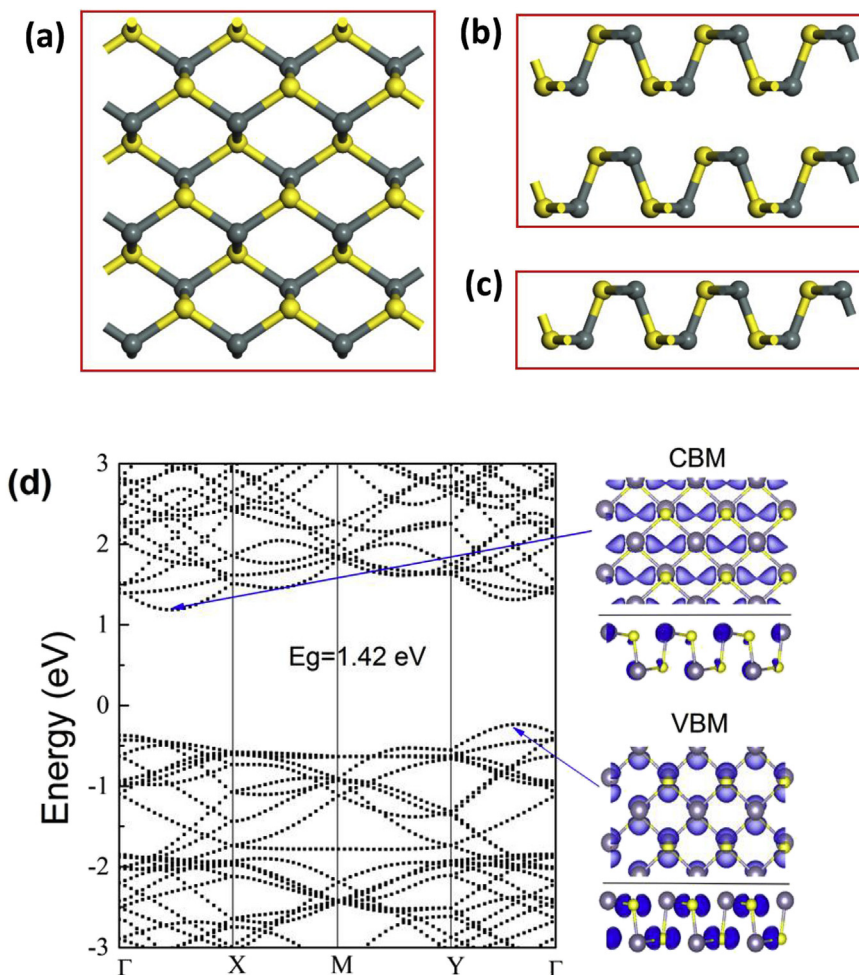


Fig. 1. (a) Top view of 3D bulk SnS/SnS monolayer. (b), (c) Side view of 3D bulk SnS/SnS monolayer. (d) Calculated band structures and partial charge density of 2D SnS monolayer.

answer to this question, the six representative configurations of Li atom that decorated SnS are included in our research as shown in Fig. 2c. According to equation (1), the adsorption energy of a Li atom adsorbed on the SnS monolayer can be obtained. Based on our calculation, the value of E_b ranges from -2.06 eV to -1.96 eV. As shown in Table 1, the values are much larger than that which Li adsorbs on the monolayer graphene (1.04 eV) [55], which guarantees a rapid loading process and strong binding between the SnS monolayer and Li atoms. Table 1, shows that H1, H2 and H3 are equivalent positions, while H4, H5 and

Table 1
Computed Li binding energies (E_b) in electronvolts for all examined Li adsorption sites on SnS monolayer.

Site	H1	H2	H3	H4	H5	H6
E_b	-1.96	-1.96	-1.96	-2.06	-2.06	-2.06

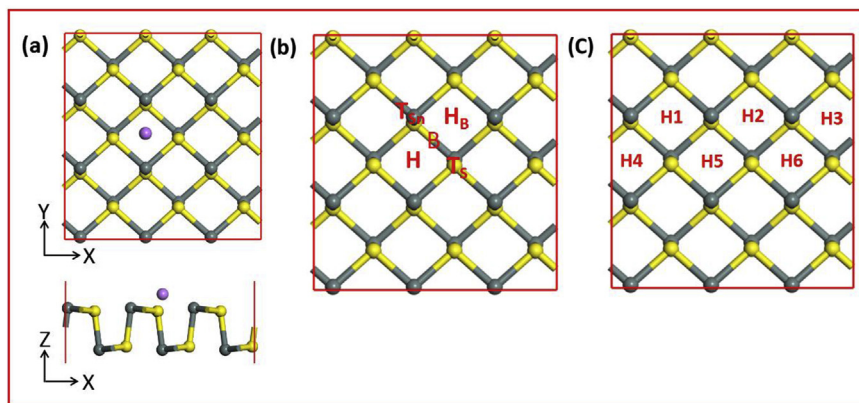


Fig. 2. (a) Top and side views of Li atom doping on SnS monolayer. (b) Four possible sites of Li atom doping on SnS monolayer. (c) H1 to H6 denote the representative sites for Li atom to be adsorbed on SnS monolayer.

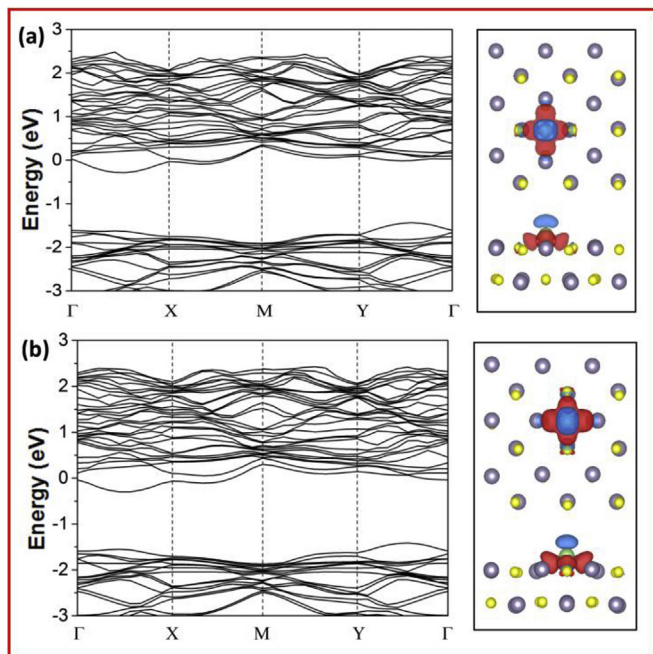


Fig. 3. Calculated band structures and differential charge density with an isosurface value of $0.02 \text{ e}/\text{\AA}^3$ of SnS monolayer with Li adsorbed (a) on H5 site, (b) on H2 site. The red and blue regions indicate an increase and decrease in electron density, respectively. (For interpretation of the references to colour in this figure legend, the reader is referred to the Web version of this article.)

H6 are equivalent positions. These data indicate that there are two kinds of lowest partial energy positions on the SnS monolayer, and we chose H2 and H5 as two typical positions.

Although a pristine SnS monolayer is a semiconductor with an indirect energy gap, the adsorption of Li atoms will significantly modify the electronic structure. As shown in Fig. 3, the SnS monolayer undergoes a semiconductor-to-metal transition upon lithiation. By means of differential charge density analysis (Fig. 3), we can see significant electron transfers from Li atom to the SnS monolayer, leading to the

semiconductor-to-metal transition. Our research indicates that Li atoms can bind to the SnS monolayer with moderate binding energies at an average of about 2.0 eV. Moreover, from the calculated electronic structures and differential charge density, adsorption of Li on H5 or H2 sites does not show significant difference.

On the other hand, the charging and circuit rate performance of the Li battery is mainly determined by Li mobility on the electrode material. It is desirable to quantify the diffusion of Li atom on the surface of SnS monolayer. In this section, we discussed the diffusion of a single Li atom on SnS monolayer. First of all, we explored the diffusion of Li on the SnS monolayer between two neighboring H sites. Since there are two different kinds of hexagon ring, we selected six representative diffusive pathways: H1→H2, H1→H5, H1→H4, H1→H3, H2→H4 and H2→H6 as indicated in Fig. 4a. After transition-states calculation, we obtained the following results: Li atom can move easily from H1 to H2/H4, whereas the energy barrier values of H1 to H3/H5 are so large that the lithium atoms cannot move straight from H1 to H3/H5. Therefore, the path of lithium atoms from H1 to H5 has to go through H2/H4 (Fig. 4b). The computed migration barriers of the Li atoms that diffuse on the SnS monolayer are about 0.45 eV, close to that of graphene [56]. It has been well explored that the diffusion barrier determines the charging/discharging process for LIBs. From the calculated energy barrier (0.45 eV), which is a suitable diffusion barrier for LIBs, we suggest that the SnS monolayer could be a potential anode material for LIBs.

Open-circuit-voltage data are widely used for characterizing the performance of Li batteries, such as state-of-charge and state-of-health. According to equation (2), the open circuit voltage curve can be obtained by calculating the binding energy defined here, which can also be interpreted as the open circuit voltage (OCV) used in battery fields if the entropy effects are neglected. Here, the calculated average voltage is about 1.98 V, which is obviously higher than those of graphite [45] and TiO₂ electrodes [46], for which the average voltage is around 1.5 V. Thus, the SnS monolayer-based Li battery is able to provide a much higher charging voltage, which is in agreement with experimental reports [44].

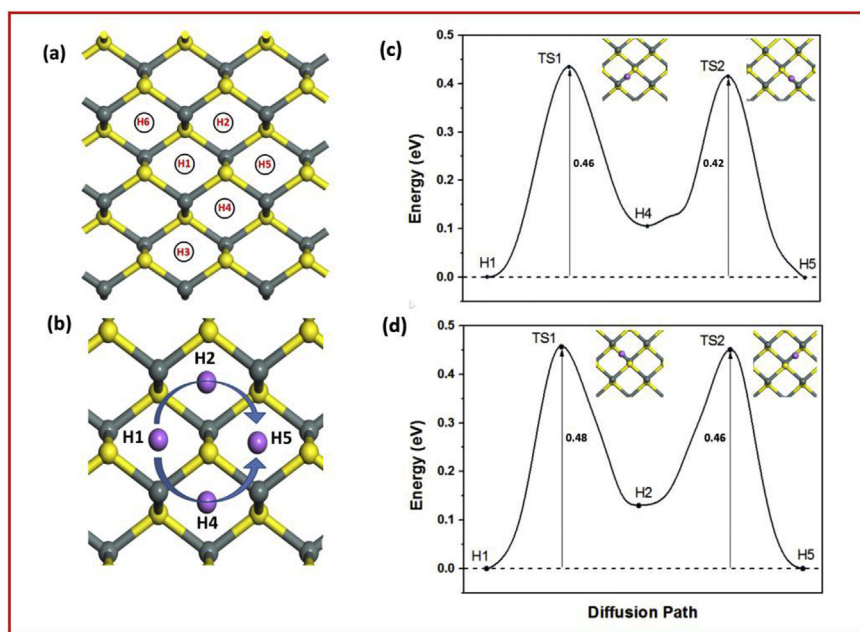


Fig. 4. (a) Six representative sites for Li atom to be adsorbed on SnS monolayer. (b) Two diffusive pathways of lithium atoms from H1 to H5. (c, d) Diffusion barriers of Li atom on SnS monolayer from H1 to H5.

4. Conclusions

To summarize, we performed DFT computations to disclose the Li adsorption and diffusion on SnS monolayer. Our results demonstrated that Li atoms can bind to the SnS monolayer with a binding energy about 2.0 eV. The SnS monolayer undergoes a transition from semiconductor to metal upon Li adsorption, which dopes electrons into the SnS monolayer. Also, for Li atom diffusion, the calculated energy barrier is around 0.45 eV, which indicates the possibility of fast charging. Furthermore, the average voltage of Li intercalation is estimated to be 1.98 V, which is suitable for high charging voltage applications. On the basis of our present findings, SnS monolayer is expected to be a promising candidate as anode material for LIBs.

Acknowledgments

This work was supported by the NSFC (11474165, 11204137), by NSF of Jiangsu Province (BK20131420), the Outstanding Youth Fund of Nanjing Forestry University (NLJQ2015-03). We also acknowledge the support from the Shanghai Supercomputer Centre.

References

- [1] X. Liu, D. Chao, Q. Zhang, H. Liu, H. Hu, J. Zhao, Y. Li, Y. Huang, J. Lin, Z.X. Shen, *Sci. Rep.* 5 (2015) 15665.
- [2] J. Wang, S. Liu, X. Zhang, X. Liu, X. Liu, N. Li, J. Zhao, Y. Li, *Electrochim. Acta* 213 (2016) 663–671.
- [3] J. Wang, L. Zhang, X. Liu, X. Zhang, Y. Tian, X. Liu, J. Zhao, Y. Li, *Sci. Rep.* 7 (2017) 41088.
- [4] N.S. Choi, Z. Chen, S. Freunberger, X. Ji, Y. Sun, K. Amine, G. Yushin, L. Nazar, J. Cho, P. Bruce, *Angew. Chem. Int. Ed.* 51 (2012) 9994–10024.
- [5] J. Liu, P. Kopold, P. van Aken, J. Maier, Y. Yu, *Angew. Chem. Int. Ed.* 54 (2015) 9632–9636.
- [6] J. Liu, K. Song, C. Zhu, C. Chen, P. van Aken, J. Maier, Y. Yu, *ACS Nano* 8 (2014) 7051–7059.
- [7] J. Liu, K. Song, P. van Aken, J. Maier, Y. Yu, *Nano Lett.* 14 (2014) 2597–2603.
- [8] Sharmistha Karmakar, C. Chowdhury, A. Datta, *J. Phys. Chem. C* 120 (27) (2016) 14522–14530.
- [9] Deutsch, Springer Neth. (2002) 357–367.
- [10] E. Buiel, J. Dahn, *Electrochim. Acta* 45 (1999) 121–130.
- [11] H. Shimoda, B. Gao, X.P. Tang, A. Kleinhammes, L. Fleming, Y. Wu, O. Zhou, *Phys. Rev. Lett.* 88 (2001) 015502.
- [12] B. Gao, C. Bower, J. Lorentzen, L. Fleming, A. Kleinhammes, X. Tang, L. McNeil, Y. Wu, O. Zhou, *Chem. Phys. Lett.* 327 (2000) 69–75.
- [13] G.T. Wu, C.S. Wang, X.B. Zhang, H.S. Yang, Z.F. Qi, P.M. He, W.Z. Li, *J. Electrochem. Soc.* 146 (1999) 1696–1701.
- [14] C.K. Chan, H. Peng, G. Liu, K. McIlwrath, X.F. Zhang, R.A. Huggins, Y. Cui, *Nat. Nanotechnol.* 3 (2008) 31–35.
- [15] A.M. Chockla, J.T. Harris, V.A. Akhavan, T.D. Bogart, V.C. Holmberg, C. Steinhagen, C.B. Mullins, K.J. Stevenson, B.A. Korgel, *J. Am. Chem. Soc.* 133 (2011) 20914–20921.
- [16] J. Hao, Y. Yang, J. Zhao, X. Liu, F. Endres, C. Chi, B. Wang, X. Liu, Y. Li, *Nanoscale* 9 (2017) 8481–8488.
- [17] X. Liu, D. Chao, Y. Li, J. Hao, X. Liu, J. Zhao, J. Lin, H.J. Fan, Z.X. Shen, *Nanomater. Energy* 17 (2015) 43–51.
- [18] K. Sugawara, K. Kanetani, T. Sato, T. Takahashi, *AIP Adv.* 1 (2011) 022103.
- [19] M.A. Romero, A. Iglesias-García, E.C. Goldberg, *Phys. Rev. B* 83 (2011) 125411.
- [20] X. Liu, D. Chao, D. Su, S. Liu, L. Chen, C. Chi, J. Lin, Z.X. Shen, J. Zhao, L. Mai, Y. Li, *Nanomater. Energy* 37 (2017) 108–117.
- [21] X. Liu, D. Zhan, D. Chao, B. Cao, J. Yin, J. Zhao, Y. Li, J. Lin, Z. Shen, *J. Mater. Chem.* 2 (2014) 12166.
- [22] X. Liu, J. Liu, D. Zhan, J. Yan, J. Wang, D. Chao, L. Lai, M. Chen, J. Yin, Z. Shen, *RSC Adv.* 3 (2013) 11601.
- [23] X. Zhao, C.M. Hayner, M.C. Kung, H.H. Kung, *ACS Nano* 5 (2011) 8739–8749.
- [24] S.P. Koenig, R.A. Doganov, H. Schmidt, A.H.C. Neto, B. Ozyilmaz, *Appl. Phys. Lett.* 104 (2014) 103106.
- [25] S. Das, M. Demarteau, A. Roelofs, *ACS Nano* 8 (2014) 11730–11738.
- [26] X. Fan, W. Zheng, J.L. Kuo, D.J. Singh, *ACS Appl. Mater. Interfaces* 5 (2013) 7793–7797.
- [27] C. Chowdhury, S. Karmakar, A. Datta, *ACS Energy Lett.* 1 (1) (2016) 253–259.
- [28] W. Li, Y. Yang, G. Zhang, Y. Zhang, *Nano Lett.* 15 (2015) 1691–1697.
- [29] Q. Yao, C. Huang, Y. Yuan, Y. Liu, S. Liu, K. Deng, E. Kan, *J. Phys. Chem. C* 119 (2015) 6923–6928.
- [30] J.R. Brent, D.J. Lewis, T. Lorenz, E.A. Lewis, N. Savjani, S.J. Haigh, G. Seifert, B. Derby, P. O'Brien, *J. Am. Chem. Soc.* 137 (2015) 12689–12696.
- [31] M. Buscema, D.J. Groenendijk, S.I. Blanter, G.A. Steele, H.S.J. vander Zant, *Nano Lett.* 14 (2014) 3347–3352.
- [32] J. Qiao, X. Kong, Z.X. Hu, F. Yang, W. Ji, *Nat. Commun.* 5 (2014) 4475.
- [33] E. Samuel Reich, *Nature* 506 (2014) 19.
- [34] V. Tran, L. Yang, *Phys. Rev. B* 89 (2014) 245407.
- [35] R. Hu, H.Y. Zhang, J.W. Liu, D.C. Chen, L.C. Yang, M. Zhu, M.L. Liu, *J. Mater. Chem. A* 3 (2015) 15097–15107.
- [36] B. Qu, C. Ma, G. Ji, C. Xu, J. Xu, Y.S. Meng, T. Wang, J.Y. Lee, *Adv. Mater.* 26 (2014) 3854–3859.
- [37] J. Seo, J. Jang, S. Park, C. Kim, C. Park, J. Cheon, *Adv. Mater.* 20 (2008) 4269–4273.
- [38] J. Wang, J. Liu, H. Xu, S. Ji, J. Wang, Y. Zhou, P. Hodgson, Y. Li, *J. Mater. Chem. A* 1 (2013) 1117–1122.
- [39] Y. Zhang, J. Lu, S. Shen, H. Xu, Q. Wang, *Chem. Commun.* 47 (2011) 5226–5228.
- [40] D. Vaughn, O.D. Hentz, S. Chen, D. Wang, R. E, *Chem. Commun.* 48 (2012) 5608–5610.
- [41] J. Kang, J.G. Park, D.W. Kim, *Electrochem. Commun.* 12 (2010) 307–310.
- [42] J. Liu, Y. Wen, P.A. van Aken, J. Maier, Y. Yu, *Nano Lett.* 14 (2014) 6387–6392.
- [43] M. Nassary, *J. Alloy. Comp.* 398 (2005) 21–25.
- [44] J. Liu, M. Gu, L. Ouyang, H. Wang, L. Yang, M. Zhu, *ACS Appl. Mater. Interfaces* 8 (2016) 8502–8510.
- [45] Y. Jing, Z. Zhou, C.R. Cabrera, Z. Chen, *J. Phys. Chem. C* 117 (2013) 25409–25413.
- [46] Z. Yang, D. Choi, S. Kerisit, K. Rosso, D. Wang, J. Zhang, G. Graff, J. Liu, *J. Power Sources* 192 (2) (2009) 588–598.
- [47] J.P. Perdew, K. Burke, M. Ernzerhof, *Phys. Rev. Lett.* 77 (1996) 3865.
- [48] G. Kresse, J. Furthmüller, *Phys. Rev. B* 54 (1996) 11169.
- [49] J. Monkhorst, J.D. Pack, *Phys. Rev. B* 13 (1976) 5188.
- [50] M. Aydinol, A.F. Kohan, G. Ceder, K. Cho, J. Joannopoulos, *Phys. Rev. B* 56 (1997) 1354–1365.
- [51] G. Henkelman, H. Jonsson, *J. Chem. Phys.* 113 (2000) 9978.
- [52] G. Henkelman, B. Uberuaga, H. Jónsson, *J. Chem. Phys.* 113 (2000) 9901.
- [53] G. Mills, H. Jónsson, *Phys. Rev. Lett.* 72 (1994) 1124.
- [54] G. Mills, H. Jónsson, G.K. Schenter, *Surf. Sci.* 324 (1995) 305–337.
- [55] C. Uthaisar, V. Barone, J.E. Peralta, *J. Appl. Phys.* 106 (2009) 113715.
- [56] C. Uthaisar, V. Barone, *Nano Lett.* 10 (8) (2010) 2838–2842.